Solubilities of Ethylene and Carbon Dioxide Gases in Lithium-ion Battery Electrolyte

Mel Soto[1], Kae Fink[1], Christof Zweifel[1], Peter J. Weddle[1], Evan Walter Clark Spotte-Smith[2,3], Kristin A. Persson[2,4], Andrew M. Colclasure[1], Bertrand J. Tremolet de Villers[1,*]

[1] National Renewable Energy Laboratory (NREL), 15013 Denver West Parkway, Golden, CO 80401, United States of America

[2] Department of Materials Science and Engineering, University of California, Berkely, CA 94720, United States of America

[3] Materials Science Division, Lawerence Berkeley National Laboratory, Berkeley, CA 94720, United States of America

[4] Molecular Foundry, Lawerence Berkeley National Laboratory, Berkeley, CA 94720, United States of America

E-mail: *bertrand.tremolet@nrel.gov

Abstract. During operation of a Li-ion battery, (electro)chemical side reactions occur within the cell that can either promote or degrade its performance. These complex reactions result in byproducts in the solid, liquid, and gas phases and must be better understood to optimize battery lifetimes. Importantly, to relate the measured gas-phase byproducts to species dissolved in the liquid-phase, equilibrium proprieties such as the Henry's Law constants are required. The present work implements a pressure decay experiment to determine the thermodynamic equilibrium concentrations between the gas and liquid phases for ethylene (C_2H_4) and carbon dioxide (CO_2), two commonly produced gases in Li-ion batteries, with an electrolyte of 1.2 M $LiPF_6$ in 3:7 wt:wt ethylene carbonate:ethyl methyl carbonate and 3 wt% fluoroethylene carbonate as a function of starting pressure. The experimental pressure decay curve is fit to an analytical dissolution model and extrapolated to predict the final pressure at equilibrium. The relationship between the partial pressures and concentration of dissolved gas in electrolyte at equilibrium is then used to determine Henry's Law constants of $k = 0.0034$ mol L^{-1} psi^{-1} for C_2H_4 and $k = 0.007$ mol L^{-1} psi^{-1} for CO_2. These values are compared to Henry's Law constants predicted from density functional theory and show good agreement within a factor of 3.

Submitted to: *Journal of The Electrochemical Society*

1. Introduction

Li-ion batteries are currently one of the most energy-dense commercial battery chemistries, dominating the market for electronic devices, electric automotives, and stationary energy storage [1, 2, 3]. However, further energy density improvements are required to electrify markets such as flight, freight, and maritime transport [1, 2, 3, 4]. In pursuit of next-generation batteries with even higher energy densities, new chemistries for anodes, cathodes, and electrolytes are continuously being investigated. At present, some of the materials receiving the most interest and scrutiny include silicon or lithium metal as replacements for graphite anodes [5, 6, 7, 8, 9], lithium-, manganese-, and nickel-rich cathodes [10, 11], and ether-based localized high-concentration electrolytes [12]. However, these materials have yet achieved mass commercialization due to significant shortcomings in cycle and/or calendar lifetimes as a result of unstable reactivities between the electrodes and the electrolyte.

A stable, electronically passivating, and ion-permeable solid-electrolyte interphase (SEI) is a key feature of Li-ion batteries, as it protects the electrode from continuous side reactions with the electrolyte while enabling Li-ion transport. While various additives, usually liquids, have been explored to improve the stability and permeability of anode SEIs, relatively little research has been done to determine the role of gases in the performance of commercial Li-ion battery chemistries, let alone next-generation battery compositions [5, 13]. Many gases are generated during Li-ion battery cycling, any of which could have possible beneficial or harmful effects on performance. Early work on Li-metal anode and Li-graphite anode batteries explored CO_2 as an additive, finding it improved cycling efficiency [14, 15, 16, 17] and stability of the graphite SEI [14, 18, 19]. These beneficial consumptive effects of CO_2 are typically associated with a more favorable SEI through the suppression of transesterification reactions and production of more cross-linked polyethylene oxide (PEO)-type polymeric species.[20, 16] More recently, Blaubaum et al. studied Li-ion batteries containing electrolyte saturated with CO_2, CO, C_2H_4, C_2H_2, H_2, CH_4, and O_2 (all gases that are commonly reported in Li-ion batteries), and concluded that battery electrolytes saturated with CO_2 and O_2 showed higher C-rate capabilities and less irreversible capacity loss during the first cycle [13].

Gas-phase byproducts typically result from electrochemical oxidation/reduction of the electrolyte solvent species. In our electrolyte system, fluoroethylene carbonate (FEC) has the highest reduction potential, and thus is most likely to decompose, first into LiF and species such as vinylene carbonate (VC).[21, 22] Ideally, the formation of a gas species could be used as a signature of a particular electrolyte species reduction, if the reaction mechanisms for electrolyte decomposition are known.[23] For example, CO is typically attributed as a byproduct from the reduction of EMC and subsequent transesterification to diethyl carbonate (DEC) and dimethyl carbonate

(DMC) [24, 22, 25]. As mentioned above, the presence of CO_2 is generally reported to have favorable effects on the cycle life [17, 26, 16]. However, competing pathways are sufficiently complex that attributing a particular gas-phase product to a certain liquid-phase reactant has proven difficult. When trying to untangle the influence of a particular species on reaction pathways, it is important to consider whether dissolved species are preferentially retained in the electrolyte or expelled away from the electrode into the reduction-free gas phase. For example, if the thermodynamics of CO_2 enable greater stability as a gas-phase species compared to a dissolved liquid-phase species, reaction mechanisms involving CO_2 consumption in the bulk, liquid electrolyte would be less likely.

To understand the availability of a particular gaseous species at the electrode interface to form the SEI, the gas species solubility in the electrolyte must be known. The solubility of ethylene in dimethyl carbonate (DMC) has been studied previously [27, 28], but ethylene solubility in other common battery solvents such as ethylene carbonate (EC) and ethyl methyl carbonate (EMC) has not been reported. The solubility of a gas is unique to a specific electrolyte formulation. Additionally, studies on CO_2 solubility indicate that the addition of Li salts such as $LiPF_6$ can also increase the solubility of the gas [29, 30].

Solubility can be determined through Henry's Law, a thermodynamic relation which relates the concentration of a gas in a liquid to the pressure of the gas above the liquid with the Henry's law constant k. Henry's Law relates gas steady-state partial pressure to solubility through,

$$c_{\text{sat}} = kP_{\text{eq}}, \tag{1}$$

where c_{sat} is the saturated gas solubility in mol L^{-1}, and k is the Henry's Law constant in mol L^{-1} psi^{-1}. Experimentally, the constant can be calculated by monitoring the pressure decay of a gas above a liquid until a steady state is reached. The measured change in pressure corresponds to the concentration of gas in the saturated liquid at the final steady state.

In the present study, an apparatus and associated methodology are presented to determine the solubilities of carbon dioxide and ethylene gases in a battery electrolyte by measuring the pressure change during dissolution of the gasses into the liquid.

2. Materials and Methods

Pressure decay trials

The pressure decay experiments were conducted in a custom-built stainless-steel Swagelok cell, modified from a design developed by Oak Ridge National Laboratory (cf., **Figure A1**).[31] The pressure was monitored using the an Omega PX-409 USBH

pressure transducer. At the start of each pressure-decay trial, the entire cell was evacuated to approximately 0.85 psia, and then filled with the target gas to the desired pressure. Three filling pressures were chosen:18, 28, and 40 psia. After gas filling, a needle valve was closed to trap gas in the gas reservoir. The other side of the cell was opened to allow the remaining gas to escape and remained open as the apparatus was cycled through an antechamber into a glovebox under argon atmosphere.

Inside the glovebox, 2 mL of electrolyte (1.2 M $LiPF_6$ dissolved in 3:7 wt:wt ethylene carbonate to ethyl methyl carbonate and 3 wt% fluoroethylene carbonate; hereafter referred to as GenF3) were added into the electrolyte reservoir using a syringe with an 18 gauge, 8" needle. The argon pressure in the box was recorded and a ball valve was closed to seal the cell. The cell was brought out of the glovebox and placed into a temperature-controlled chamber at 30 °C. The cell was allowed to rest for two hours to allow the internal pressure to equilibrate. This equilibrated value was recorded as P_{gr} and indicates the pressure of the gas reservoir before the trial began. The needle valve was then fully opened to release the target gas into the electrolyte chamber. The pressure decay over time was recorded in 3 s intervals on the Omega Transducer software.

Accurate volume measurements of the entire cell were needed to calculate the moles of gas present in the system during the trials. This was done separately using a difference-in-mass method with deionized water. During volume measurements, the transducer was replaced by a solid steel national pipe tapered thread (NPT) plug, which was tightened to the same position as the transducer. The cell with all valves open was fully dried at 80 °C overnight in a vacuum oven, then cooled and weighed empty. It was filled with water through the electrolyte reservoir, capped, and then reweighed. This was repeated 5 times and the mass differences were averaged and converted to volume using the density of water.

Pressure decay modeling

Pressure decay by mass transfer is a slow process, resulting in a need for a model to extrapolate the final equilibrium pressure, P_{eq}. The pressure decay of a gas dissolving into a liquid through mass transfer was modeled by Behzadfar et al. [32] and results in the analytical expression given by:

$$P = P_{\mathrm{eq}} + \frac{8 c_{\mathrm{sat}} Z_{\mathrm{g}} R T V_{\mathrm{l}}}{\pi^2 V_{\mathrm{g}}} \sum_{n=1}^{\infty} \frac{1}{(2n-1)^2} \exp\left(-(2n-1)^2 \frac{\pi^2}{4L^2} D t\right), \qquad (2)$$

where P is the measured pressure, c_{sat} is the saturation concentration, Z_{g} is the gas compressibility (0.99426 and 0.99 for C_2H_4 and CO_2, respectively), V_{l} is the volume of the liquid (2.0 mL), D is the species liquid-phase diffusivity, L is the diffusion length (7.02 mm), R is the universal gas constant, T is the temperature, and V_{g} is the volume

of the gas (12.78 mL). Equation 2 solves for the pressure at time t, and notably does not model the initial pressure drop due to the interface filling phenomenon that occurs at the beginning of the experiment [32]. To use this expression, our datasets exclude this early-stage pressure drop to obtain a more accurate regression. It is assumed that the electrolyte, prepared only in the glovebox, has little to no C_2H_4 or CO_2 gas dissolved it in to begin with. The datasets are fit to Eq. 2 by iteratively solving for the final pressure, P_{eq}, and the diffusivity D that minimize the sum of squares of the error differences between the experimental and model data points (i.e., least squares regression fitting).

After all trials at the same gas reservoir pressure had concluded and been modeled, their diffusivities were averaged and input back into Eq. 2. The fit was then determined by keeping D constant and only varying P_{eq}. These final produced P_{eq} values were used for subsequent solubility calculations and the construction of the Henry's Law curve.

In addition to measuring the Henry's Law constant, the Henry's Law constant is also predicted using density functional theory (DFT). All DFT calculations used the Q-Chem electronic structure code version 5[33] with the ωB97X-V range-separated hybrid generalized gradient approximation exchange-correlation functional[34] and the def2-TZVPPD basis set.[35] Some optimized structures and free energies for molecules in solvent were taken from the Lithium Ion Battery Electrolyte (LIBE) dataset.[25] In LIBE, solvent effects are treated implicitly using the solvent model with density (SMD),[36] using parameters relevant to a 3:7 mixture of ethylene carbonate (EC) and ethyl methyl carbonate (EMC); for molecules not included in LIBE, we have been consistent with this choice in solvent model and parameters. The solvent-optimized structures were then re-optimized in vacuum to obtain the gas-phase thermochemistry.

From these DFT calculations, the solvation free energy $\Delta G_{solvation}$ is calculated as

$$\Delta G_{\text{solvation}} = G_{\text{EC/EMC}} - G_{\text{vacuum}}, \tag{3}$$

where $\Delta G_{\text{EC/EMC}}$ is the free energy of the molecule in the solution phase (using SMD) and ΔG_{vacuum} is the free energy of the molecule in vacuum. From $\Delta G_{\text{solvation}}$, the Henry's law coefficient k can be expressed as

$$k = RT \exp\left(\Delta G_{\text{solvation}}/RT\right). \tag{4}$$

DFT calculations using SMD can predict the solvation free energies of small molecules with high accuracy. When calculating the solvation free energies of neutral molecules in one of the 90 nonaqueous solvents included in its training set, SMD achieves a mean unsigned error of 0.67 kcal mol^{-1} (0.03 eV).[36] While one might reasonably expect a somewhat higher error when calculating solvation free energies in solvents outside of the training set, such as 3:7 EC/EMC, the thermodynamics obtained from DFT should nonetheless be reasonably accurate for the types of small gases considered here. However, calculating Henry's Law coefficients is considerably more challenging as

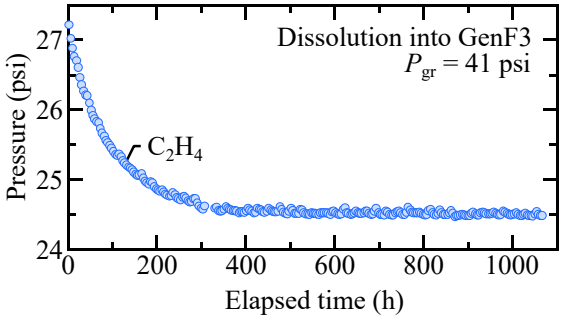

Figure 1. A pressure decay curve of ethylene dissolution into GenF3 with P_{gr} = 41 psia concluded at $t = 1060$ h.

compared to computing the solvation free energies. As seen in Eq. 4, calculating the Henry's Law coefficient requires exponentiation of the solvation free energy, meaning even very small errors in $\Delta G_{solvation}$ can have a considerable impact on the predicted coefficient. As an example, modifying $\Delta G_{solvation}$ by 1 kcal mol^{-1} would cause k to change by a factor of roughly 5.4.

3. Results

Figure 1 illustrates a long-term trial of C_2H_4 dissolution in GenF3 with a gas reservoir initial pressure, P_{gr} = 41 psia. After the needle valve is opened, the gas escapes the reservoir and fills the entire cell, which causes a sharp pressure drop due to expansion of the gas into the part of the cell containing electrolyte (the headspace above the liquid). This is followed by a steep initial pressure decay, attributed to the interface-filling phenomenon as the gas saturates the topmost layers of the liquid in the reservoir [32]. The value of the initial pressure, P_i, is calculated after the needle valve is opened at $t = 0$ s, but before the interface filing occurs assuming ideal gas behavior (i.e., $P = nRT/V_g$). The final value P_{eq} is an average of the last 20 measured data points before the trial was stopped. The initial and equilibrium partial pressures of the gas are used to accurately calculate the change in moles moving from the gas phase to the solution phase.

Equation 2 was also used to extrapolate the P_{eq} of shorter trials (<150 h) that were concluded before equilibrium was reached. To best approximate the behavior of the slow pressure decay due to dissolution, the data sets used in the model are in seconds and begin where $dP/dt < 0.005$ Δpsi s^{-1}, after the interface-filling regime. To determine an optimal time for the conclusion of the trials, the t = 1060 h data set was used to calculate the model-fit percent error in P_{eq} when the trial runtime length was varied. **Figure 2** shows the decreasing percent error with data sets of increasing trial runtime. After 96 h the percent error is consistently less than 1%. There is some

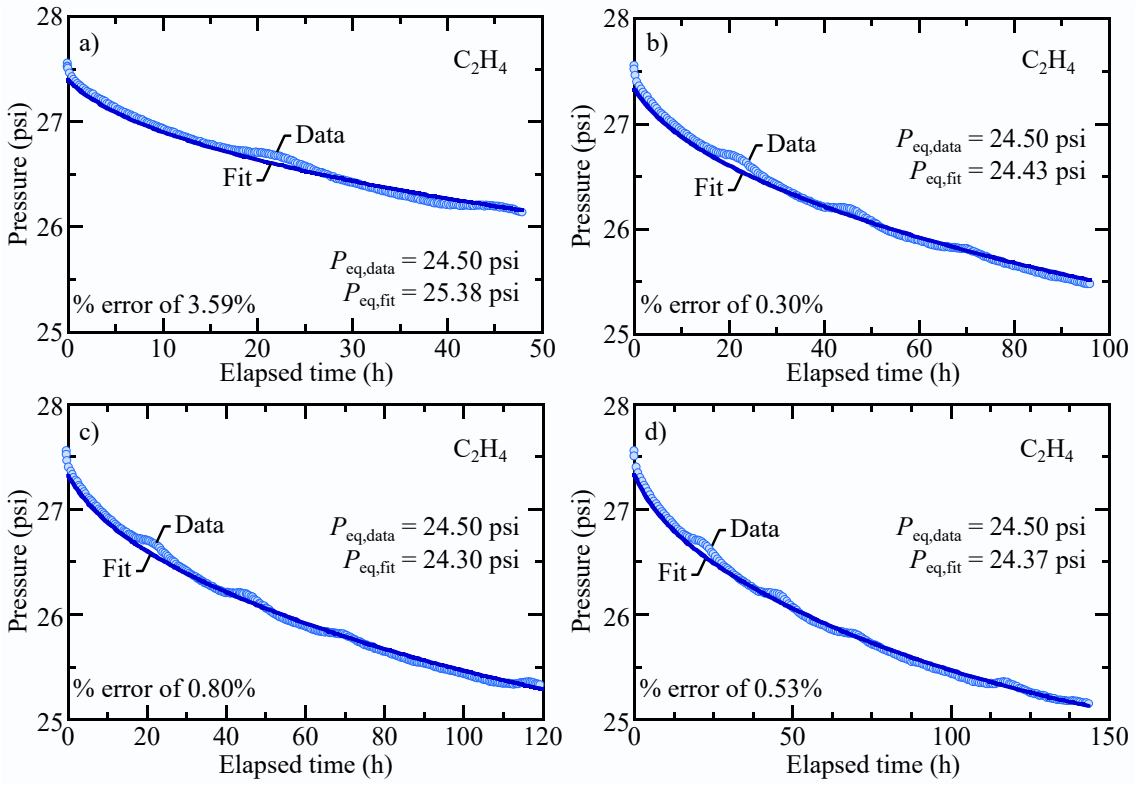

Figure 2. Experimental and model fit pressure decay curves of the t = 1060 h solubility trial of C_2H_4, ending at a) 48 h, b) 96 h, c) 120 h, and d) 144 h. Each trial produces a P_{eq} from the fit that is compared to the experimental P_{eq} by calculating P.

systematic noise in Fig. 2 that appear as "bumps" in the data appearing approximately 24 h apart. This systematic error is attributed to daily temperature changes in the room.

Figure 3 shows the experimental and best fit curves for a C_2H_4 and a CO_2 trial at $P_{gr} = 28$ psi. The fits have a coefficient of determination, $R^2 > 0.99$, for both gases. Although Behzadfar et al. studied the diffusivity of CO_2 in bitumen,[32] that R^2 is very close to 1 for both gases studied here, despite large differences in decay rates, emphasizes the accuracy of the chosen model for a carbonate-based battery electrolyte.

Figure 4 illustrates the solubility with respect to partial pressure for (a) C$_2$H4 and (b) CO_2. The slope of the lines is the Henry's Law constant. The plots illustrate both the experimentally measured data and the DFT-predicted (labelled "Theory") trends. For the gases studied in this work, the Henry's Law coefficients predicted by DFT differ from the experimental values by factors of 1.53 and 2.92 for C_2H_4 and CO_2, respectively. This discrepancy implies that the error in the predicted solvation free energy is at most 0.63 kcal mol^{-1} (0.03 eV), which is well within "chemical accuracy" (of 1 kcal mol^{-1}).

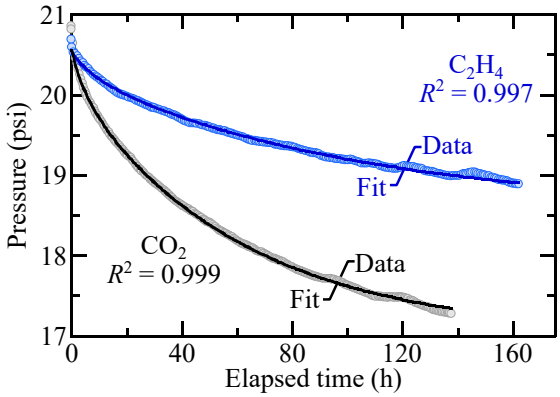

Figure 3. Experimental and model fit pressure decay curves with R^2 comparisons for CO_2 and C_2H_4 at P_{gr} of 28 psi.

In part, the observed error between theory and experiment may arise because the SMD parameters used in this study to calculate k did not account for the effect of FEC nor the $LiPF_6$ salt, which may impact the solvation free energy of small molecules. However, we attribute the error in calculated solvation free energy primarily to the fundamental limitations of implicit solvent models. As mentioned, SMD performs well on a variety of neutral small molecules in organic solvents, but it is nonetheless known to fail to capture certain effects, for instance ionic and hydrogen bonding [37]. Calculating solvation free energies using explicit solvation shells, rather than an implicit solvent medium, may provide an opportunity to achieve better agreement with experiment.

4. Discussion

The present work describes an experimental procedure to measure the solubility of gasses in a widely-used lithium-ion battery electrolyte by monitoring the pressure change of a gas as it dissolves into the liquid electrolyte. The gases in this study were chosen because they readily form via (electro)chemical reactions during normal operation of an Li-ion battery during cell formation. While the time to reach equilibrium pressure and saturation gas concentration is typically 500-1000 h, it is shown here that a complex multi-phase model allows extrapolation to equilibrium with measurements lasting $<$ 100 h. As the equilibrium constant for a given gas species is highly influenced by the electrolyte composition, including the salt concentration, it would be intractable to measure many different gas/electrolyte equilibrium concentrations without the approach described in this work.

This work also demonstrates the calculation of Henry's Law constants for these gas phase species in carbonate electrolyte, enabling the determination of their equilibrium dissolved concentrations. We anticipate that this will allow researchers to

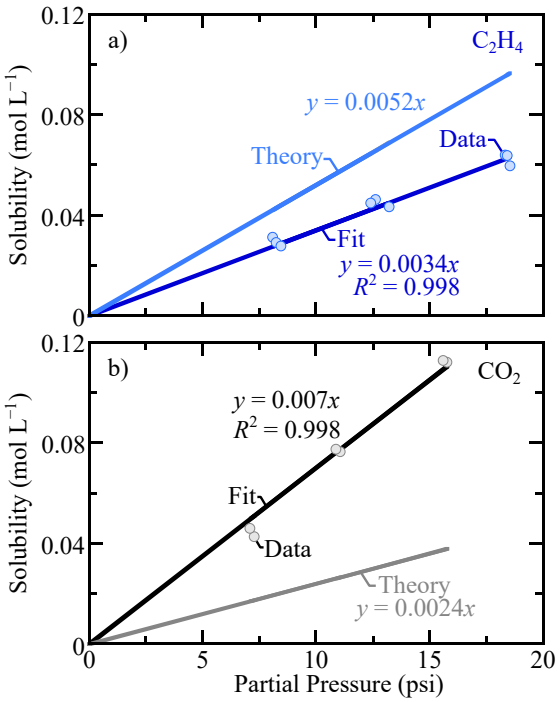

Figure 4. Experimental and theoretical Henry's law curves of a) C_2H_4 and b) CO_2

better interrogate the complex, competing reaction pathways, including gas reactants, occurring in Li-ion batteries, particularly within the SEI. Furthermore, there are relatively few Henry's Law constants reported in the literature in battery-relevant systems [27, 28]. Thus, there is an inherent need to measure and report the Henry's Law constants for predominate gas species in common Li-ion battery electrolytes.

Additionally, the thermodynamic calculations from DFT are validated by comparison to experimentally determined Henry's Law constants for the two gaseous species studied (CO_2 and C_2H_4) in this work. The DFT-predicted and measured Henry's Law constants were found to agree well, with small errors $\leq$ 0.63 kcal mol^{-1}. This indicates that current theoretical models can predict Henry's Law constants within an order of magnitude, potentially even without accounting for every species in solution. However, further improvements can still be made, and there is a need to develop physics-based models that can accurately determine these constants to extrapolate these results to future/unique electrolyte systems.

5. Conclusions

The pressure decay at different starting pressures of C_2H_4 and CO_2 gas dissolving into GenF3 battery electrolyte was recorded and modeled to extrapolate the equilibrium

pressures, P_{eq}. Analysis of trial run time was conducted, determining the minimum trial length of 96 h to minimize percent error of the model fit P_{eq}. The differences in moles from initial to equilibrium partial pressures were used to calculate the solubility of each gas at the equilibrium pressures, and this was done for several initial pressures. The equilibrium pressures versus solubility were plotted to calculate the Henry's Law constants k for each gas with $k_{C_2H_4}$ of 0.0034 mol L^{-1} psi^{-1} and k_{CO_2} of 0.007 mol L^{-1} psi^{-1}. Using the Environmental Protection Agency (EPA) standards, these two species would be considered "volitile" in the electrolyte studied [38, 39]. This means that the species are significantly more stable in the gas-phase as compared to the liquid-phase. In terms of studying reaction mechanisms that form SEI species, there is a significant competing pathway to eject these dissolved species to the gas-phase as compared to retain these species to feed additional reaction cascades. Nevertheless, the equilibrium saturation concentrations of both C_2H_4 and CO_2 are estimated to be in the range of tens of mmol L^{-1} at reasonable partial pressures expected for a typical Li-ion battery, suggesting that an appreciable amount of gas remains in the liquid that could contribute to electrochemical side reactions during cell operation.

These experimental constants were compared to theoretical k constants in 3:7 EC:EMC solution. Despite the DFT calculations not including salt coordination or FEC effects, the predicted constants differed by factors of 1.53 and 2.92 for C_2H_4 and CO_2, respectively. Differences between experimental measurements and DFT calculations are attributed to limitations of the DFT solvent models and presence of additives in the EC:EMC experimental solution.

Although only two gases were measured in this study, our approach will be extended to several others — CO, C_2H_2, H_2, CH_4, and O_2 — that are typically formed during formation and cycling of a lithium-ion battery. Furthermore, additional electrolyte formulations will be explored to quantify effects on gas solubility of varying solvent, liquid additives, and salt concentrations.

6. Acknowledgements

This work is authored in part by the National Renewable Energy Laboratory, operated by Alliance for Sustainable Energy, LLC, for the U.S. Department of Energy (DOE) under Contract No. DE-AC36-08GO$_2$8308. This research was supported by the U.S. Department of Energy's Vehicle Technologies Office under the Silicon Consortium Project, directed by Brian Cunningham and managed by Anthony Burrell.

This work was also supported in part by the U.S. Department of Energy, Office of Science, Office of Workforce Development for Teachers and Scientists (WDTS) under the Science Undergraduate Laboratory Internships Program (SULI).

Additional support is provided by the Kavli Energy NanoScience Institute

Philomathia Graduate Student Fellowship (E.W.C.S.-S.). Data for this study was produced using computational resources provided by the National Energy Research Scientific Computing Center (NERSC), a U.S. Department of Energy Office of Science User Facility under Contract No. DE-AC02-05CH11231, the Eagle HPC system at the National Renewable Energy Laboratory (NREL), and the Lawrencium HPC cluster at Lawrence Berkeley National Laboratory.

Appendix A

Fig. A1 depicts the custom apparatus designed to measure pressure decays. See Section 2 for details of the apparatus and the measurement protocols.

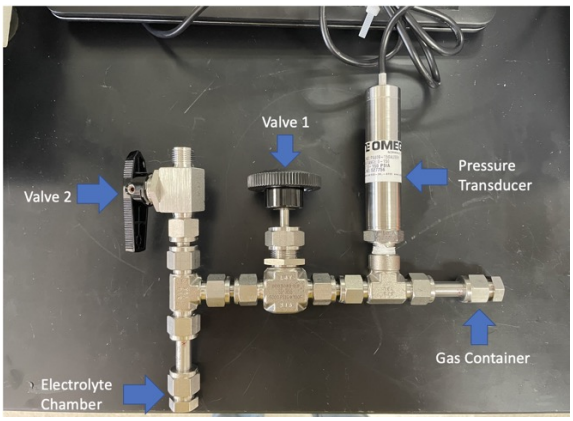

Figure A1. Swagelok solubility cell used in the pressure decay experiments. Valve 1 is the needle valve that is closed to trap gas in the gas reservoir. Valve 2 is the ball valve used to seal the entire cell after electrolyte has been added into the electrolyte chamber.

References

[1] Armand M and Tarascon J M 2008 *Nature* **451** 652–657 ISSN 1476-4687 URL https://doi.org/10.1038/451652a https://www.nature.com/articles/451652a.pdf

[2] Placke T, Kloepsch R, Dúhnen S and Winter M 2017 *J. Solid State Electrochem.* **21** 1939–1964 ISSN 1433-0768 URL https://doi.org/10.1007/s10008-017-3610-7 https://link.springer.com/content/pdf/10.1007/s10008-017-3610-7.pdf

[3] Dunn B, Kamath H and Tarascon J M 2011 *Science* **334** 928–935 URL https://www.science.org/doi/abs/10.1126/science.1212741 https://www.science.org/doi/pdf/10.1126/science.1212741?download=true

[4] Eshetu G, Zhang H, Judez X, Adenusi H, Armand M, Passerini S and Figgemeier E 2021 *Nat. Commun.* **12** 5459 ISSN 2041-1723 URL https://doi.org/10.1038/s41467-021-25334-8 https://www.nature.com/articles/s41467-021-25334-8.pdf

[5] Eshetu G and Figgemeier E 2019 *ChemSusChem* **12** 2515–2539 ISSN 1864-5631 URL https://onlinelibrary.wiley.com/doi/abs/10.1002/cssc.201900209 https://onlinelibrary.wiley.com/doi/pdf/10.1002/cssc.201900209

[6] McBrayer J, Rodrigues M T, Schulze M, Abraham D, Apblett C, Bloom I, Carroll G, Colclasure A, Fang C, Harrison K, Liu G, Minteer S, Neale N, Veith G, Johnson C, Vaughey J, Burrell A and Cunningham B 2021 *Nat. Energy* **6** 866–872 ISSN 2058-7546 URL https://www.nature.com/articles/s41560-021-00883-w

[7] Schulze M, Rodrigues M T, McBrayer J, Abraham D, Apblett C, Bloom I, Chen Z, Colclasure A, Dunlop A, Fang C, Harrison K, Liu G, Minteer S, Neale N, Robertson D, Tornheim A, Trask S, Veith G, Verma A, Yang Z and Johnson C 2022 *J. Electrochem. Soc.* **169** 050531 ISSN 1945-7111 0013-4651 URL https://dx.doi.org/10.1149/1945-7111/ac6f88 https://iopscience.iop.org/article/10.1149/1945-7111/ac6f88/pdf

[8] Liu B, Zhang J G and Xu W 2018 *Joule* **2** 833–845 ISSN 2542-4351 URL https://www.sciencedirect.com/science/article/pii/S2542435118300977

[9] Liu J, Bao Z, Cui Y, Dufek E, Goodenough J, Khalifah P, Li Q, Liaw B, Liu P, Manthiram A, Meng Y, Subramanian V, Toney M, Viswanathan V, Whittingham M, Xiao J, Xu W, Yang J, Yang X Q and Zhang J G 2019 *Nat. Energy* **4** 180–186 ISSN 2058-7546 URL https://doi.org/10.1038/s41560-019-0338-x https://www.nature.com/articles/s41560-019-0338-x.pdf

[10] Sun Y K 2019 *ACS Energy Lett.* **4** 1042–1044 doi: 10.1021/acsenergylett.9b00652 URL https://doi.org/10.1021/acsenergylett.9b00652

[11] Gutierrez A, Tewari D, Chen J, Srinivasan V, Balasubramanian M and Croy J 2023 *J. Electrochem. Soc.* **170** 030509 ISSN 1945-7111 0013-4651 URL https://dx.doi.org/10.1149/1945-7111/acbee4 https://iopscience.iop.org/article/10.1149/1945-7111/acbee4/pdf

[12] Cao X, Jia H, Xu W and Zhang J G 2021 *J. Electrochem. Soc.* **168** 010522 ISSN 1945-7111 0013-4651 URL https://dx.doi.org/10.1149/1945-7111/abd60e https://iopscience.iop.org/article/10.1149/1945-7111/abd60e/pdf

[13] Bláubaum L, Röse P, Schmidt L and Krewer U 2021 *ChemSusChem* **14** 2943–2951 ISSN 1864-564X URL https://onlinelibrary.wiley.com/doi/abs/10.1002/cssc.202100845 https://chemistry-europe.onlinelibrary.wiley.com/doi/full/10.1002/cssc.202100845

[14] Plichta E, Slane S, Uchiyama M, Salomon M, Chua D, Ebner W and Lin H 1989 *J. Electrochem. Soc.* **136** 1865 ISSN 1945-7111 0013-4651 URL https://dx.doi.org/10.1149/1.2097063 https://iopscience.iop.org/article/10.1149/1.2097063/pdf

[15] Chusid O, Ein Ely E, Aurbach D, Babai M and Carmeli Y 1993 *J. Power Sources* **43** 47–64 ISSN 0378-7753 (Youngman)

[16] Hopkins E, Frisco S, Pekarek R, Stetson C, Huey Z, Harvey S, Li X, Key B, Fang C, Liu G, Yang G, Teeter G, Neale N and Veith G 2021 *J. Electrochem. Soc.* **168** 030534 ISSN 1945-7111 URL https://dx.doi.org/10.1149/1945-7111/abec66

[17] Krause L J, Chevrier V L, Jensen L D and Brandt T 2017 *J. Electrochem. Soc.* **164** A2527 ISSN 1945-7111 URL https://dx.doi.org/10.1149/2.1121712jes https://iopscience.iop.org/article/10.1149/2.1121712jes

[18] Aurbach D, Ein-Eli Y, Chusid O, Carmeli Y, Babai M and Yamin H 1994 *J. Electrochem. Soc.* **141** 603 ISSN 1945-7111 0013-4651 (Youngman) URL https://dx.doi.org/10.1149/1.2054777 https://iopscience.iop.org/article/10.1149/1.2054777/pdf

[19] Ein-Eli Y, Markovsky B, Aurbach D, Carmeli Y, Yamin H and Luski S 1994 *Electrochim. Acta* **39** 2559–2569 ISSN 0013-4686

[20] Strehle B, Solchenbach S, Metzger M, Schwenke K U and Gasteiger H A 2017 *J. Electrochem. Soc.* **164** A2513–A2526 URL http://jes.ecsdl.org/lookup/doi/10.1149/2.1001712jes

[21] Hou T, Yang G, Rajput N N, Self J, Park S W, Nanda J and Persson K A 2019 *Nano Energy* **64** 103881 ISSN 22112855 URL http://www.sciencedirect.com/science/article/pii/S2211285519305877

[22] Weddle P, Spotte-Smith E, Verma A, Patel H, Fink K, de Villers B T, Schulze M, Blau S, Smith K, Persson K and Colclasure A 2023 *Electrochim. Acta* **accepted**

[23] Seitzinger C L, Sacci R L, Coyle J E, Apblett C A, Hays K A, Armstrong R R, Rogers A M, Armstrong B L, Bennet T H, Neale N R and Veith G M 2020 *Chem. Mater.* **32** 3199–3210 ISSN 0897-4756 URL https://doi.org/10.1021/acs.chemmater.0c00308 https://pubs.acs.org/doi/full/10.1021/acs.chemmater.0c00308

[24] Fang C, Tran T N, Zhao Y and Liu G 2021 *Electrochim. Acta* **399** 139362 ISSN 0013-4686 URL https://www.sciencedirect.com/science/article/pii/S0013468621016522

[25] Spotte-Smith E, Blau S, Xie X, Patel H, Wen M, Wood B, Dwaraknath S and Persson K 2021 *Sci. Data* **8**

[26] Chevrier V, Krause L, Jensen L, Huynh C, Triemert M, Bowen E and Thorson J 2018 *J. Electrochem. Soc.* **165** A2968 ISSN 1945-7111 URL https://dx.doi.org/10.1149/2.0351813jes

[27] de la Iglesia O, Mainar A, Pardo J I and Urieta J 2003 *J. Chem. Eng. Data* **48** 657–661 ISSN 0021-9568 doi: 10.1021/je020199q URL https://doi.org/10.1021/je020199q https://pubs.acs.org/doi/pdf/10.1021/je020199q

[28] Terrado E, Pardo J, Urieta J and Mainar A 2005 *J. Chem. Eng. Data* **50** 512–516 ISSN 0021-9568 doi: 10.1021/je0496894 URL https://doi.org/10.1021/je0496894

[29] Dougassa Y, Jacquemin J, El Ouatani L, Tessier C and Anouti M 2014 *J. Phys. Chem. B* **118** 3973–3980 cited By :39 Export Date: 19 July 2022 URL https://pubs.acs.org/doi/pdf/10.1021/jp500063c

[30] Dougassa Y, Jacquemin J, El Ouatani L, Tessier C and Anouti M 2014 *J. Chem. Thermodyn.* **79** 49–60 ISSN 00219614

[31] Browning K L, Baggetto L, Unocic R R, Dudney N J and Veith G M 2013 *J. Power Sources* **239** 341–346 ISSN 0378-7753 URL https://doi.org/10.1016/j.jpowsour.2013.03.118

[32] Behzadfar E and Hatzikiriakos S 2014 *Energy Fuels* **28** 1304–1311 ISSN 0887-0624 URL https://doi.org/10.1021/ef402392r https://pubs.acs.org/doi/pdf/10.1021/ef402392r

[33] Epifanovsky E, Gilbert A, Feng X, Lee J, Mao Y, Mardirossian N, Pokhilko P, White A, Coons M, Dempwolff A, Gan Z, Hait D, Horn P, Jacobson L, Kaliman I, Kussmann J, Lange A, Lao K, Levine D, Liu J, McKenzie S and et al 2021 *J. Chem. Phys.* **155** 084801

[34] Mardirossian N and Head-Gordon M 2014 *Phys. Chem. Chem. Phys.* **16** 9904–9924

[35] Rappoport D and Furche F 2010 *J. Chem. Phys.* **133** 134105

[36] Marenich A, Cramer C and Truhlar D 2009 *J. Phys. Chem. B* **113** 6378–6396

[37] Zhang J, Zhang H, Wu T, Wang Q and van der Spoel D 2017 *J. Chem. Theory Comput.* **13** 1034–1043

[38] McAtee M, Johnson J, Hauschild V and et al 2010 *Methodology for developing chemical exposure guidelines for deployed military personnel* U.S. Army Public Health Command available at https://phc.amedd.army.mil/PHC%20Resource%20Library/RD230%20June%202010%20Revision.pdf

[39] Murphy B and Morrison R 2007 *Introduction to environmental forensics* (Elsevier)